Influence of Lipid Composition on Physical Properties and PEG-Mediated Fusion of Curved and Uncurved Model Membrane Vesicles: "Nature's Own" Fusogenic Lipid Bilayer†

Md. Emdadul Haque,‡ Thomas J. McIntosh,§ and Barry R. Lentz*,‡

Department of Biochemistry & Program in Molecular/Cell Biophysics, University of North Carolina, Chapel Hill, North Carolina 27599-7260, and Department of Cell Biology, Duke University Medical Center, Durham, North Carolina 27710

Received August 28, 2000; Revised Manuscript Received February 9, 2001

ABSTRACT: Poly(ethylene glycol) (PEG)-mediated fusion of phosphatidylcholine model membranes has been shown to mimic the protein-mediated biomembrane process [Lee, J., and Lentz, B. R. (1998) *Proc. Natl. Acad. Sci. U.S.A. 95*, 9274−9279]. Unlike the simple model membranes used in this earlier study, the lipid composition of fusogenic biomembranes is quite complex. The purpose of this paper was to examine PEG-mediated fusion of highly curved (SUV) and largely uncurved (LUV) membrane vesicles composed of different lipids in order to identify lipid compositions that produce highly fusogenic membranes. Starting with liposomes composed of five lipids with different physical properties, dioleoylphosphatidylcholine (DOPC), dioleoylphosphatidylethanolamine (DOPE), dioleoylphosphatidylserine (DOPS), bovine brain sphingomyelin (SM), and cholesterol (CH), we systematically varied the composition and tested for the extent of PEG-mediated fusion after 5 min of treatment. We found that a vesicle system composed of four lipids, DOPC/DOPE/SM/CH, fused optimally at a 35/30/15/20 molar ratio. Each lipid seemed to play a part in optimizing the membrane for fusion. PE disrupted outer leaflet packing as demonstrated with TMA-DPH lifetime, C_6-NBD-PC partitioning, and DPH anisotropy measurements, and thus significantly enhanced fusion and rupture, without significantly altering interbilayer approach (X-ray diffraction). An optimal ratio of PC/PE (35/30) produced a balance between fusion and rupture. CH and SM, when present at an optimal ratio of 3/4 in vesicles containing the optimal PC/PE ratio, reduced rupture without significantly reducing fusion. This optimal CH/SM ratio also enhanced outer leaflet packing, suggesting that fusion is dependent not only on outer leaflet packing but also on the properties of the inner leaflet. Addition of CH without SM enhanced rupture relative to fusion, while SM alone reduced both rupture and fusion. The optimal lipid composition is very close to the natural synaptic vesicle composition, suggesting that the synaptic vesicle composition is optimized with respect to fusogenicity.

The lipid compositions of natural membranes are complex, with different lipids likely having different roles in membrane function. Phosphatidylcholine (PC),[1] one of the major lipid species of mammalian membranes, forms a stable bilayer. Its relatively strongly hydrated headgroup inhibits fusion in model membranes (*1*). Phosphatidylethanolamine (PE), a second major component of mammalian membranes, has a cone-shaped molecular structure and the ability to promote the bilayer-to-hexagonal phase transition that may facilitate membrane fusion (*2*). Sphingomyelin (SM) has a molecular shape and hydration properties similar to PC, but, in the presence of cholesterol, SM is thought (*3, 4*) to be involved in domain formation and be enriched in detergent-resistant membranes or "rafts" (*5, 6*). SM also forms a stoichiometric (1/1) complex with cholesterol (CH) (*7, 8*). Cholesterol (CH) is present in most mammalian membranes, but in very different amounts in different organelles (*9*). Although CH appears to have several different functions in eukaryotic cells, two of its primary and essential roles are to decrease permeability and increase the stability of membrane bilayers.

Membrane fusion is of fundamental importance in the life of a cell. It is a major process mediated by proteins in which a major rearrangement of lipid structures must occur in a limited region of interbilayer contact. Many aspects of bilayer structure and lipid physical properties are thought to contribute to the fusion process, such as bilayer dehydration (*10*), imperfect lipid packing (*11, 12*), local alterations in bilayer curvature (*13, 14*), outer leaflet packing defects (*12*), elastic free energy (*15*), changes in membrane fluidity (*10, 16*), and locally induced nonbilayer phases (*17*). Lipid

† Supported by USPHS Grants GM 32707 to B.R.L. and GM 27278 to T.J.M.

* To whom correspondence should be addressed (uncbrl@med.unc.edu).

‡ University of North Carolina.

§ Duke University Medical Center.

[1] Abbreviations: SUVs, small, unilamellar vesicles made by sonication; LUVs, large, unilamellar vesicles made by extrusion; QELS, quasi-elastic light scattering; DOPC, 1,2-dioleoyl-3-*sn*-phosphatidylcholine; DOPE, 1,2-dioleoyl-3-*sn*-phosphatidylethanolamine; DOPS, 1,2-dioleoyl-3-*sn*-phosphatidylserine; SM, sphingomyelin (bovine brain); CH, cholesterol; C_6-NBD-PC, 1-palmitoyl-2-*N*-(4-nitrobenz-2-oxa-1,3-diazole)aminohexanoylphosphatidylcholine; DPH, 1,6-diphenyl-1,3,5-hexatriene; TMA-DPH, 1-[4-(trimethylammonium)-6-phenyl]-1,3,5-hexatriene; Tb^{3+}, terbium; DPA, pyridine-2,6-dicarboxylic acid; TES, *N*-[tris(hydroxymethyl)methyl]-2-aminoethanesulfonic acid; PEG, poly(ethylene glycol); $C_{12}E_8$, dodecyloctaethylene glycol monoether; SIN, Sindbis virus; SFV, Semliki forest virus; HIV, human immunodeficiency virus.

10.1021/bi002030k CCC: $20.00
Published on Web 03/16/2001

composition can affect any and all of these. Specific proteins in different membranes play a crucial role in directing and catalyzing fusion, but fusogenicity is highly dependent on the lipid composition of the target membrane. Fusion of influenza virus peptide (*18*) and human immunodeficiency virus peptide (HIV[1]) (*19*) with their target cells is significantly increased by the presence of negatively charged lipids in the target membrane. Fusion of Semliki virus (SFV[1]) and Sindbis virus (SIN[1]) correlates with the CH and SM content of the target membrane (*20, 21*), while fusion of Sendai virus (*22*) and vesicular stomatitis virus (*23*) is correlated with the cholesterol content of the target membrane. Other systems are dependent on unsaturated PE (*2*). The presence of CH in the target membrane is necessary for SFV and SIN virus binding, and subsequent fusion is regulated by sphingolipids (*24*).

To understand the mechanism of membrane fusion in biological systems, researchers have used mainly simple model systems composed of one or two lipid classes (e.g., PS, PC, PC/PE, PC/PS). Very little is known about the fusion of model membranes with complex lipid compositions (e.g., PC/PE/SM/PI/PS, PC/PE/SM/PS/PI/PA/CH, and PC/PE/SM/CH) (*25*−*27*). A detailed study of the sensitivity of membrane fusion to the broad complexity of biomembrane composition would be challenging at the least. The aim of this report is to begin this process by addressing the influence of several basic classes of lipids on the extent of poly(ethylene glycol)-mediated model membrane fusion. To choose the lipid classes on which to focus, we sought to compare to the composition of a highly fusogenic natural membrane, the synaptic vesicle. If we ignore differences between ether- and ester-linked lipids, the synaptic vesicle membrane can roughly be considered to contain five lipid classes: PC, PE, PS (representing acidic phospholipids PS and phosphatidic acid), SM, and CH. To find a fusogenic vesicle composition, we systematically evaluated PEG-mediated membrane fusion of model membrane vesicles with different proportions of these five lipids. These studies have defined an optimal model membrane composition for the fusion process and have shed light on the role of each lipid class in contributing to the fusion process. A remarkable result is that the optimal composition we have defined has PC, PE, SM, and CH in nearly the same ratio in which they are observed in synaptic membrane vesicles.

EXPERIMENTAL PROCEDURES

Materials

Chloroform stock solutions of 1,2-dioleoyl-3-*sn*-phosphatidylcholine (DOPC[1]), 1,2-dioleoyl-3-*sn*-phosphatidylethanolamine (DOPE[1]), 1,2-dioleoyl-3-*sn*-phosphatidylserine (DOPS[1]), sphingomyelin (bovine brain, SM[1]), and 1-palmitoyl-2-*N*-(4-nitrobenz-2-oxa-1,3-diazole)aminohexanoylphosphatidylcholine (C_6-NBD-PC[1]) were purchased from Avanti Polar Lipids, Inc. (Birmingham, AL), and used without further purification. The concentration of all the stock lipids was determined by phosphate assay (*28*). Cholesterol (CH[1]) was purchased from Avanti Polar Lipids and was further purified as previously reported by Schwenk et al. (*29*). 1,6-Diphenyl-1,3,5-hexatriene (DPH) and 1-[4-(trimethylammonium)-6-phenyl]-1,3,5-hexatriene (TMA-DPH[1]) were purchased from Molecular Probes (Eugene, OR). Terbium (Tb^{3+}) chloride was purchased from Johnson Matthey Co. (Ward Hill, MA). Dipicolinic acid (DPA[1]) and *N*-[tris(hydroxymethyl)methyl]-2-aminoethanesulfonic acid (TES[1]) were purchased from Sigma Chemical Co. (St. Louis, MO). Poly(ethylene glycol) of molecular weight 7000−9000 (PEG[1] 8000) was purchased from Fisher Scientific (Fairlane, NJ) and further purified as previously reported (*30*). Dodecyloctaethylene glycol monoether ($C_{12}E_8$[1]) was purchased from Calbiochem (La Jolla, CA). Deuterium oxide (99.8% deuterated) was purchased from Aldrich Chemical Co. (Milwaukee, WI). All other reagents were of the highest purity grade available.

Methods

Vesicle Preparation. Small, unilamellar vesicles were prepared as reported by Lentz et al. (*14*). Mixtures of different lipids at appropriate molar ratios in chloroform were dried under nitrogen. The dried mixed lipids were dissolved in 1 mL of cyclohexane containing a small aliquot of methanol, frozen in a shell on the surface of a small vial using dry ice, and dried under high vacuum overnight. The dried lipids were suspended in an appropriate buffer for 1 h above the main phase transition. The phase transition temperatures of the lipid mixtures were measured using DPH anisotropy (*31*). For SUV preparation, the lipid suspension was sonicated using a Heat Systems model 350 sonicator (Plainview, NY) equipped with a titanium probe tip. Vesicles were fractionated by centrifugation at 70 000 rpm for 25 min at 4 °C using a Beckman TL-100 ultracentrifuge (Palo Alto, CA). Large, unilamellar vesicles (LUVs) of different compositions were prepared by the extrusion method (*32, 33*). Multilamellar lipid suspensions were extruded 10 times through a 0.1 μm polycarbonate filter (Nucleo Pore Corp., Pleasanton, CA) at room temperature under a pressure of 100 psi of N_2. Details of this method are described in an earlier publication (*30*). For TMA-DPH and C_6-NBD-PC lifetime measurements, vesicles were prepared in buffer containing 100 mM NaCl, 1 mM EDTA, and 2 mM TES at pH 7.4.

Contents Mixing and Leakage Assay. The Tb/DPA contents mixing and leakage assays were based on those originally proposed by Wilschut et al. (*34*) and adapted to monitor PEG-induced fusion as described in Talbot et al. (*35*). Buffers contained 185 mM NaCl, 3.7 mM L-His, 3.7 mM TES, 20 mM $CaCl_2$, and 2.0 mM Na_2EDTA for the Tb^{3+}/DPA (excitation at 278 nm and emission at 545 nm) contents mixing and leakage assays, as documented in Talbot et al. (*35*). Untrapped probe-containing buffer was removed from the vesicles using a Sephadex G-75 column equilibrated with probe-free buffer. The lipid concentration was 0.2 mM. Leakage of contents was followed using vesicles containing coencapsulated 7.5 mM $TbCl_3$ and 75 mM dipicolinic acid (DPA[1]). When leakage of contents occurred, there was a drop in fluorescence due to quenching by water (*36*) of Tb^{3+} released from complexation with DPA when the trapped compartment was diluted into the external compartment. The fluorescence intensity of the coencapsulated Tb/DPA vesicles suspended in sub-fusion PEG concentrations was taken as indicating 0% leakage. The fluorescence intensity of Tb/DPA vesicles after treatment with 0.45 mM $C_{12}E_8$ (20 μL of $C_{12}E_8$ added to 2 mL of vesicle suspension) was taken to indicate 100% leakage of trapped contents, so that: % leakage = $[\Delta F(0\text{ wt \% PEG}) - \Delta F(x\text{ wt \% PEG})]/[\Delta F(0\text{ wt \% PEG})]$,

where ΔF is the decrease in Tb/DPA fluorescence upon addition of $C_{12}E_8$.

To measure the mixing of vesicle contents due to fusion, Tb- and DPA-containing vesicles were mixed (1/1), added to a PEG solution, and incubated for 5 min at 23 °C before the fluorescence of the Tb/DPA complex was measured. Five minutes is a convenient time of incubation for moderately fusing systems, since it occurs in the midst of the overall time course, thus giving a rough measure of fusion rate (*37*). Incubating for other times would not change our conclusion, only the magnitudes of contents mixing and leakage values. Detergent was added to release the contents of the vesicles, and fluorescence intensity was once again recorded. The fluorescence of coencapsulated Tb/DPA vesicles was taken as indicative of 100% contents mixing, such that: % contents mixing (CM) = ΔF(Tb + DPA; *x* wt % PEG)]/ΔF(Tb/DPA; *x* wt % PEG)]. Details of this procedure are described by Talbot et al. (*35*).

Measurements of TMA-DPH and C_6-NBD-PC Fluorescent Lifetime. Small aliquots (0.04−0.8% of vesicle sample volumes) of a stock solution of C_6-NBD-PC (0.65 mM) in methanol were added to 0.2 mM vesicle suspensions to obtain different lipid/probe ratios. Similarly, small aliquots of a stock solution of TMA-DPH in methanol were added to 0.2 mM vesicle suspensions to achieve a lipid/probe ratio of 250/1. Samples were thoroughly stirred using a vortexer and incubated 5 min before lifetime measurements. Phase shifts and modulation ratios were collected using an SLM 48000 MHF spectrofluorometer equipped with a Coherent Inova 90 argon-ion laser (Coherent Auburn Group, Auburn, CA). The probes were excited by vertically polarized and modulated light with a wavelength of 488 nm for C_6-NBD-PC and in a region from 351.1 to 363.8 nm of the laser UV multiline for TMA-DPH. Emission light was passed through a Glan-Thomson polarizer oriented at an angle of 54.7° from the vertical and through a 2 mm OG 515 filter (Schott Optic Glass, Duryea, PA) for C_6-NBD-PC and a 3 mm KV-450 filter (Schott Optic Glass, Duryea, PA) for TMA-DPH. The dynamic data acquisition routine of the SLM 48000 MHF spectroscopy software package was used to collect phase shift and modulation ratios at 37 frequencies using a 5 s acquisition time and 300 acquisition average, and a glycogen solution as a zero lifetime reference. Phase-resolved lifetimes and mole fractions of each lifetime component were estimated using the global analysis software package supplied by SLM (Globals Unlimited, Urbana, IL).

The average lifetime was calculated from

$$\tau_{AV} = \Sigma\alpha_i\tau_i^2/\Sigma\alpha_i\tau_i \qquad (1)$$

where α_i and τ_i are the mole fraction and lifetime of the *i*th component, respectively. Lifetimes were calculated from a three-lifetime-component analysis for C_6-NBD-PC and a two-lifetime-component analysis for TMA-DPH. For C_6-NBD-PC, the lifetime of the probe in a micelle state was fixed as 1 ns, and the sum of the mole fractions of the other two components was taken as the mole fraction of the probe partitioned into the membrane (*12*).

Measurements of Deuterium Isotope Sensitivity of the Lifetime. The accessibility of water to the exchangeable protons of TMA-DPH can be estimated from the ratio of the lifetime of TMA-DPH in D_2O to the lifetime in H_2O, since a proton at this exchangeable position lowers the lifetime of the chromophore (*38*). Since the exchangeable protons of TMA-DPH are located in the headgroup region, this ratio should reflect hydration or lipid packing in the headgroup/interface region of the bilayer. A lipid/probe ratio of 250/1 was used for these measurements.

X-ray Diffraction. Two types of lipid preparations were studied by X-ray diffraction, unoriented multilamellar vesicle suspensions and oriented lipid multilayers. Multilamellar vesicles were prepared in water (10−15 mg/mL) from PC/PE/SM/CH (35/30/15/20 molar ratio) and PC/SM/CH (65/15/20 molar ratio) lipid mixtures. The vesicles were aggregated in 5% PEG, pelleted with a bench centrifuge, and sealed in quartz glass capillary tubes. The capillary tubes were mounted in a point collimation X-ray camera. Oriented multilayers were formed by drying lipid/water suspensions on a curved glass substrate and mounting the substrate in a controlled relative humidity chamber on a line-focused X-ray camera. X-ray diffraction patterns were recorded on Kodak DEF 5 X-ray film at 23 °C. For each order *h* the integrated intensity $I(h)$ was determined by densitometry as previously described (*8*, *40*), and the structure amplitude $F(h)$ was set equal to $\{hI(h)\}^{1/2}$ for the oriented specimens (*39*, *40*). Electron density profiles, $\rho(x)$, on a relative density scale were calculated from

$$\rho(x) = (2/d)\Sigma\exp\{i\phi(h)\}*F(h)*\cos(2\pi xh/d) \qquad (2)$$

where *d* is the lamellar repeat period, $\phi(h)$ is the phase angle for order *h*, and the sum is over *h*. Phase angles were assigned by comparing the diffracted intensities with continuous Fourier transforms of similar systems (*8*, *41*). Electron density profiles were calculated at a resolution of $d/2h_{max} \cong 7$ Å.

Determination of Particle Diameter. Vesicle diameters were measured by quasi-elastic light scattering (QELS) measurements using a custom-built multiangle instrument (*30*) that incorporates a computing autocorrelator from Particle Sizing Systems, Inc. (Santa Barbara, CA). Data collection and analysis were controlled by software located in an external personal computer. Vesicle size was calculated in the volume weighted mode. The detailed procedure is reported elsewhere (*41*).

RESULTS

Exploration of Fusogenicity of Vesicles with Various Compositions. Figure 1 shows the extents of contents mixing (A) and leakage (B) for SUVs of different lipid compositions as a function of PEG concentration (wt/wt %). At low percentages of PEG (up to 5 wt %), a significant amount of contents mixing was observed for PC/PE/SM/CH vesicles without any significant accompanying leakage (closed triangles). Incorporation of PS into the PC/PE/SM/CH composition led to membranes that fused well (open circles), but not to the same extent as PC/PE/SM/CH vesicles. This suggests that membrane fusion was inhibited due to the electrostatic repulsion of negatively charged surfaces. However, this drop-off in fusion occurred despite the fact that our contents mixing assay buffer contained roughly 16 mM free Ca^{2+}, which should be more than sufficient to cause interbilayer PS−Ca^{2+}−PS complex formation that should favor interbilayer approach (*42*). When we performed experiments at decreasing Ca^{2+} concentrations, fusion was

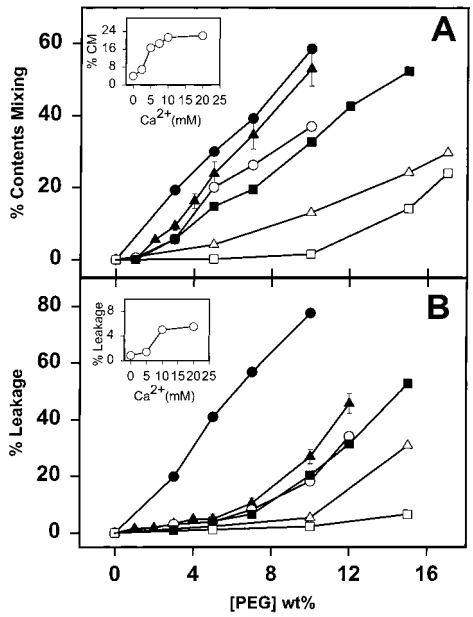

FIGURE 1: Effect of lipid composition of the fusogenicity of SUVs. Contents mixing (A) and leakage (B) were measured as described under Methods and are plotted as a function of PEG concentration (wt/wt %) at 23 °C for PC/PE/CH (43/37/20) (filled circles), PC/PE/SM/CH (35/30/15/20) (filled triangles), PC/PE (60/40) (filled squares), PC/PE/SM/PS/CH (30/25/15/10/20) (open circles), PC/PE/SM (44/37/19) (open triangles), and PC/PE/SM (55/30/15) (open squares) SUVs. Representative standard error bars are shown for the PC/PE/SM/CH data set. The insets show the influence of Ca^{2+} concentration on (A) contents mixing and (B) leakage at 5 wt % PEG in PC/PE/SM/PS/CH (30/25/15/10/20) SUVs.

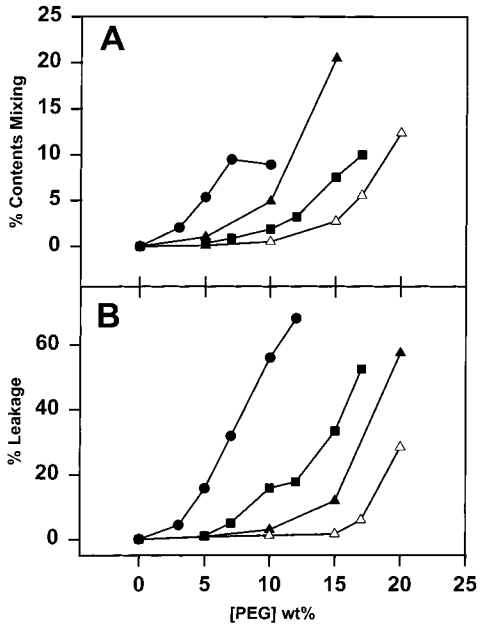

FIGURE 2: Effect of lipid composition of the fusogenicity of LUVs. Experimental conditions and symbols were the same as for Figure 1, except that large, unilamellar vesicles (LUVs) prepared by extrusion were used for contents mixing (A) and leakage (B) measurements, whose results are shown as a function of PEG concentration (wt/wt %) at 23 °C.

inhibited even more dramatically by the presence of PS (Figure 1A, inset) while leakage was reduced less (Figure 1B, inset). Thus, the presence of PS in SUVs inhibited membrane fusion dramatically. For this reason, we limit our attention from here on to neutral lipids.

Vesicles composed of PC/PE (closed squares) fused, but much less so than PC/PE/SM/CH vesicles, while leakage was similar for both lipid compositions. CH had a significant destabilizing influence on PC/PE vesicles. Unlike the other lipid systems, SUVs composed of PC/PE/CH aggregated at room temperature even in the absence of PEG. Very high apparent contents mixing was observed for PC/PE/CH vesicles (filled circles) even at 3−4 wt % PEG, but this was not actual contents mixing, since it was accompanied by significant leakage. Apparently, cholesterol without SM led to vesicles that ruptured instead of mixing their contents. SM had the opposite effect on PC/PE vesicles, in that leakage was nearly nonexistent up to 10 wt % PEG in vesicles composed of PC/PE/SM (open triangles), but contents mixing was also quite limited. It seems that SM led to very sturdy membranes that resisted rupture, but also could not fuse. The presence of CH allows SM-toughened membranes to fuse. Clearly, the lipid composition of highly curved membranes affects the ability of these membranes to fuse in a variety of ways.

We also examined membranes without significant curvature stress. PEG-mediated contents mixing (A) and leakage (B) of LUVs is shown in Figure 2. These results show that LUVs behave similarly to highly curved SUVs with respect to their lipid compositions, except that SUVs are more fusogenic, as expected (*35*).

Determination of Optimal PE/PC and SM/CH Molar Ratios for Fusion of PC/PE/SM/CH SUV. From the results presented in Figures 1 and 2, it seems that vesicles composed of mixtures of PC/PE/SM/CH provide a good balance between fusogenicity and resistance to rupture under the osmotic stress imposed by PEG. To determine a PE/PC molar ratio of PC/PE/SM/CH SUV optimal for fusion, we systematically evaluated PEG-mediated contents mixing and leakage (shown in Figure 3) at different concentrations of PEG, while holding the SM/CH ratio constant at 15/20. Fusogenicity increased with PE/PC ratio but so did bilayer instability. The extent of contents mixing and leakage increased at 40/25 (filled circles) and 35/30 (filled squares) PE/PC ratios, whereas significant contents mixing and low leakage was observed for a 30/35 PE/PC molar ratio (filled triangles). There was no contents mixing and leakage at 0% PE (open squares). Figure 4 shows the variation of contents mixing (circles) and contents leakage (triangles) as a function of PE/PC ratio at a fixed PEG concentration (7 wt/wt %) and SM/CH ratio. The inset shows the difference between contents mixing and leakage as a function of PE/PC ratio. This difference is maximal at a PE/PC molar ratio of 30/35, a ratio that apparently results in an optimal balance between fusion and rupture.

Figure 5 shows end-point fusion profiles as a function of PEG concentration for PC/PE/SM/CH SUVs with varying SM/CH molar ratios, but with the PE/PC molar ratio fixed at its optimal value of 30/35 (see Figure 4). Increasing amounts of SM significantly reduced rupture but also severely limited fusion. Once again, the playoff between rupture and fusion defined an optimum SM/CH molar ratio at 7% (w/w) PEG, as shown in Figure 6. The inset to Figure 6 shows the difference between contents mixing and leakage as a function of SM/CH ratio at the same PEG concentration. These results clearly indicate that a SM/CH ratio of 15/20

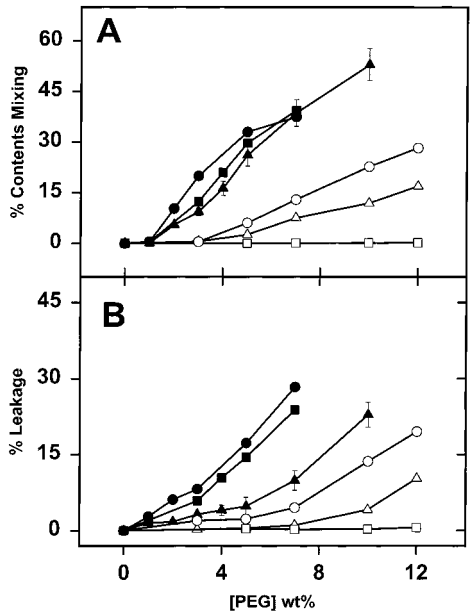

FIGURE 3: Effect of the PE/PC ratio on PEG fusion profiles. PEG-mediated contents mixing (A) and leakage (B) at 23 °C for PC/PE/SM/CH SUV are shown as a function of PEG concentration. The SM/CH ratio was held constant (15/20) as the molar ratio of PE to PC was varied: PE/PC (40/25) (filled circles); PE/PC (35/30) (filled squares); PE/PC (30/35) (filled triangles); PE/PC (25/40) (open circles); PE/PC (20/45) (open triangles); and PE/PC (0/65) (open squares).

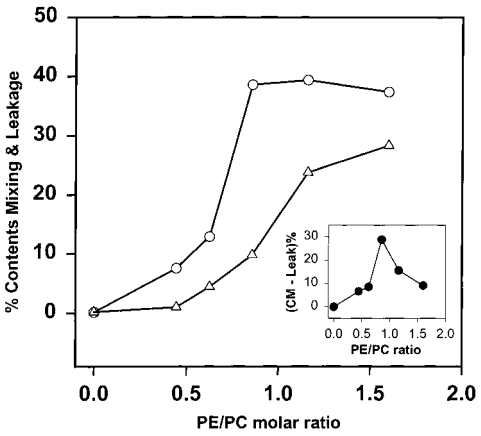

FIGURE 4: Effect of the PE/PC ratio on fusion at constant PEG. Contents mixing (circles) and leakage (triangles) are plotted as a function of the PE/PC ratio at a constant SM/CH (15/20) ratio and at a fixed PEG concentration (7% w/w). The inset shows the difference between contents mixing and leakage as a function of PE/PC ratio.

optimizes the difference between fusogenicity and rupture, at least at the optimal PE/PC ratio.

Since high curvature generally causes membranes to fuse more readily, we wanted to know whether variation of membrane curvature with vesicle composition was responsible for the optimal composition we have defined. The size distributions of vesicles of different compositions are recorded in Table 1. Not surprisingly, vesicle diameter changed with lipid composition, since different lipids have different intrinsic curvatures (see Discussion). Addition of any lipid other than PC produced slightly larger SUVs, although a mixture of SM and CH added to PC had minimal effect on vesicle diameter. The most dramatic effects of lipid composition occurred upon addition of PE or PE & CH to PC. The

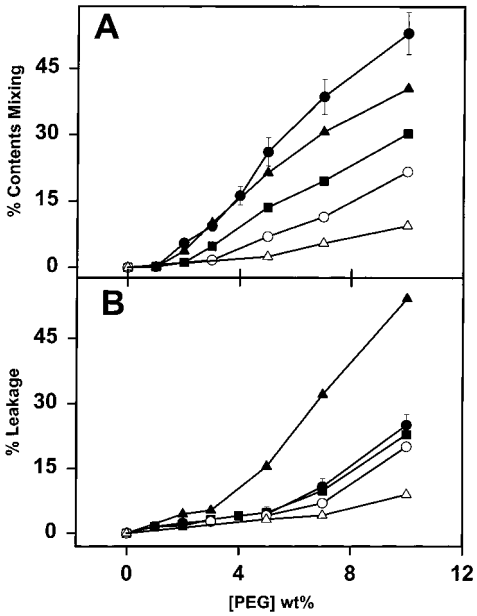

FIGURE 5: Effect of the SM/CH ratio on PEG fusion profiles. Contents mixing (A) and leakage (B) at 23 °C for PC/PE/SM/CH SUV, holding the PE/PC ratio constant (30/35), are shown for varying molar ratios of SM/CH: SM/CH (15/20) (filled circles); SM/CH (10/25) (filled triangles); SM/CH (17.5/17.5) (filled squares); SM/CH (25/10) (open circles); and SM/CH (35/0) (open triangles).

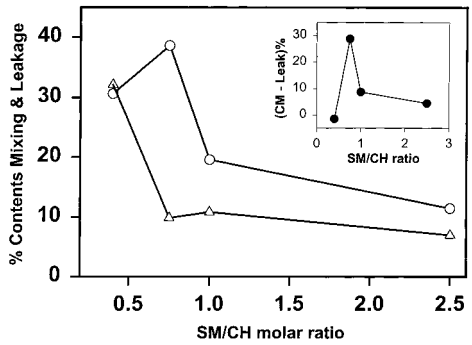

FIGURE 6: Effect of the SM/CH ratio on fusion at fixed PEG. Contents mixing and leakage for PC/PE/SM/CH SUV are shown as a function of SM/CH ratio at 7% (w/w) PEG and at a fixed PE/PC ratio (30/35). The inset shows the difference of contents mixing and leakage as a function of the SM/CH ratio.

effect of PE is not surprising, since it has a negative intrinsic curvature and would not easily accommodate to the high positive curvature of the outer leaflet of a SUV. The effect of CH is more difficult to understand, since its intrinsic curvature is slightly negative. It must be that CH somehow interferes with the ability of PE and PC to support a highly curved vesicle structure, since LUVs prepared from this lipid mixture were roughly the same size as other LUVs. This is consistent with the remarkable fragility of PC/PE/CH SUVs (Figure 1). Figure 7 shows the variation of diameters of PC/PE/SM/CH vesicles as a function of the molar ratio of PE/PC at fixed SM/CH ratio (triangles) and the molar ratio of SM/CH at fixed PE/PC (30/35) ratio (circles). SUV diameter was independent of SM/CH molar ratio at a fixed PE/PC (30/35) ratio but increased with increasing mole percent of PE at a fixed SM/CH (15/20) ratio. These results are consistent with a high concentration of PE making it increasingly difficult to produce SUVs with high positive curvature in their outer leaflets.

Table 1: Diameters of SUVs and LUVs of Different Compositions[a]

systems	distribution width	diameter (nm)	standard error	*n*
PC/PE/SM/PS/CH 30/25/15/10/20, SUV	46.8	31.2	±1.1	4
PC/PE/SM/CH 35/30/15/20, SUV	50.7	24.5	±1.3	4
PC/PE/SM 55/30/20, SUV	46.0	22.9	±1.7	3
PC/SM/CH 65/15/20, SUV	46.1	20.0		2
PC/PE/CH 43/37/20, SUV	52.1	37.5		1
PC/PE 60/40, SUV	59.7	24.4		2
PC, SUV	58.4	18.8	±0.7	3
PC/PE/SM/CH 35/30/15/20, LUV	51.3	125.8	±1.15	3
PC/PE/CH 44/37/20, LUV	51.5	126.8		2
PC/PE 60/40, LUV	49.4	121.9	±1.3	3
PC/PE/SM 55/30/20, LUV	45.2	120.2		1

[a] *n* is the number of measurements. The diameter is reported in the volume weighting mode.

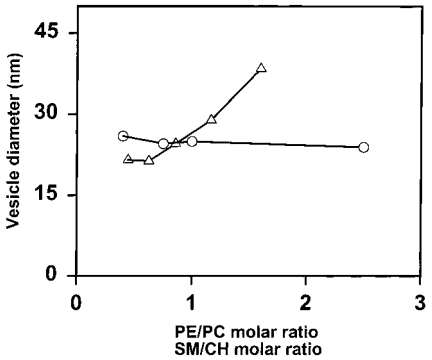

FIGURE 7: Effect of lipid composition on SUV size. Diameters of PC/PE/SM/CH vesicles are plotted as a function of the mole ratio of PE/PC at a fixed SM/CH (15/20) ratio (triangles) and of the molar ratio of SM/CH at a fixed PE/PC (30/35) ratio (circles).

TMA-DPH and DPH To Monitor Packing of Vesicle Outer Leaflets. To explore the relationship between the surface properties of the membrane and fusogenicity, we used the fluorescence properties of TMA-DPH to follow membrane packing and water penetration into the interface or backbone region of the membrane outer leaflet. TMA-DPH was added to and incubated with preformed vesicles for 5 min. Under these conditions, the probe partitions into the outer leaflet of vesicle membranes. We measured first the excited-state lifetime of this probe in H_2O and D_2O buffer (see Methods). Two lifetime components were required to fit the phase shift and modulation ratio data for TMA-DPH in SUV suspensions (lipid/probe ratio of 250/1). These were averaged as described under Methods to obtain the average lifetimes shown in Table 2. The average fluorescence lifetime of TMA-DPH in PC/PE/SM/CH SUV was much higher than that in PC/PE vesicles and slightly greater than that in PC/SM/CH vesicles. This could be due to differences in the thermal motions of the probe environment in different vesicles or to different extents of water penetration into the bilayers of the different vesicles. To focus on water penetration, we examined the ratio of lifetimes measured in D_2O to those measured in H_2O ($\tau_{AV}^{D_2O}/\tau_{AV}^{H_2O}$). Since it is tied to the aqueous phase by its charge, the probe is expected to be located in the interface region of the three different membranes (*43*). The closer the $\tau_{AV}^{D_2O}/\tau_{AV}^{H_2O}$ ratio is to 1, the less water penetrates into the interface region of the membrane outer leaflet (*43*). The results (Table 2) suggest that water penetration into the outer leaflet of PC/PE/SM/CH and PC/SM/CH SUVs was less than for PC/PE SUVs. This result is consistent with the work of Simon et al. (*44*) that showed that the presence of cholesterol decreases the depth of water penetration into lipid bilayers. The fluorescence anisotropy of DPH (Table 2) also suggested that the acyl chain region of PC/PE/SM/CH and PC/SM/CH SUVs was more ordered than for PC/PE SUVs. Based on these conclusions, it is surprising that PC/PE membranes were less fusogenic than PC/PE/SM/CH membranes (Figure 1). Also, PC/SM/CH membranes, which had outer leaflet properties very similar to those of PC/PE/SM/CH SUVs, were nonfusogenic (open squares, Figure 3). This means that fusogenicity is not dependent only on outer leaflet packing defects, and that outer leaflet packing is only one of several factors that regulates membrane fusion (*12*).

Lifetime and Partitioning of C_6-NBD-PC To Monitor Packing of the Outer Leaflets of Membranes with Different Lipid Compositions. The influence of membrane surface properties on fusogenicity was further examined using a fluorescent probe, C_6-NBD-PC, which is reported to partition into the upper region of the bilayer (*45*). The fluorescence lifetime of C_6-NBD-PC has been shown to be sensitive to lipid headgroup packing (*46*). The phase shifts and modulation ratios of C_6-NBD-PC at different lipid/probe ratios in SUV suspensions of different compositions were fitted to three lifetime components. One of these components is the probe lifetime in a micelle (1.06 ns) while the other two reflect C_6-NBD-PC partitioned into the membrane (*12*). The short lifetime is independent of lipid-to-probe ratio as well as vesicle composition. The average lifetimes and total mole fractions of C_6-NBD-PC in membranes of different lipid/probe ratios are shown in Figure 8. The average lifetime of the probe in PC/PE/SM/CH (open circles) and PC/SM/CH (open triangles) vesicles was considerably larger than that in PC/PE (open squares) SUVs. This result indicates that the local environment of the probe in PC/PE/SM/CH or PC/SM/CH membranes was either more hydrophobic or less dynamic than in PC/PE membranes. The average lifetime of the probe partitioned into PC/PE/SM/CH SUVs increased slightly with lipid/probe ratio, but increased more dramatically for PC/SM/CH and especially noticeably for PC/PE SUV with lipid/probe ratio. This suggests that the free volume available to accommodate the probe increased in the order PC/PE > PC/SM/CH > PC/PE/SM/CH SUV. The mole fractions of C_6-NBD-PC partitioning into membranes of different compositions (shown in Figure 8B) were in the same order. The mole fraction of probe partitioning into PC/PE vesicles increased substantially (30%) with lipid/probe ratio in the range from 123 to 308, but increased by only 10% for PC/SM/CH SUV and by 3% for PC/PE/SM/CH SUV in the same range of lipid/probe ratio. These results indicate that outer leaflet packing of PC/PE/SM/CH membranes was tighter than that of PC/SM/CH membranes and the packing in both these membranes was much tighter than in PC/PE membranes. This conclusion is consistent with results and conclusions based on TMA-DPH lifetime and DPH anisotropy data (Table 2).

Table 2: Fluorescence Lifetimes of TMA-DPH and Fluorescence Anisotropy of DPH for SUVs of Different Compositions[a]

systems	lipid/probe ratio	TMA-DPH lifetime ($\tau_{AV}^{H_2O}$)	TMA-DPH lifetime ($\tau_{AV}^{D_2O}$)	($\tau_{AV}^{D_2O}$)/($\tau_{AV}^{H_2O}$)	DPH anisotropy
PC/PE/SM/CH 35/30/15/20	250	4.363 ± 0.010	4.808 ± 0.011	1.101	0.165 ± 0.003
PC/SM/CH 65/15/20	250	4.052 ± 0.028	4.513 ± 0.022	1.114	0.154 ± 0.003
PC/PE 54/46	250	3.096 ± 0.027	3.608 ± 0.016	1.165	0.090 ± 0.004

[a] Lifetime error ranges were obtained from the standard deviations in fitting parameters obtained from global analysis of these data sets in terms of a two-lifetime model (see Methods).

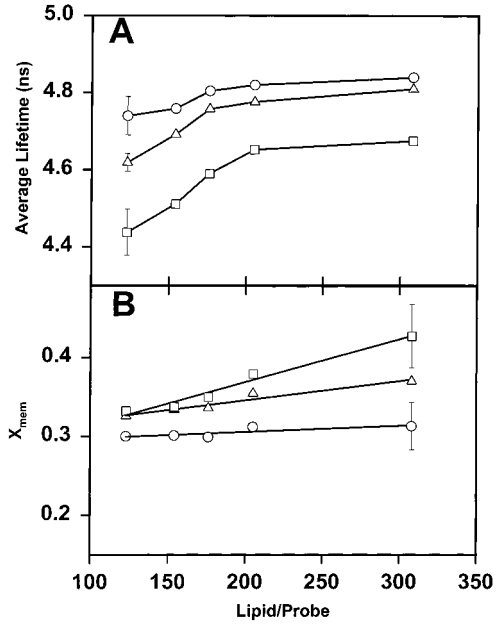

FIGURE 8: Effect of lipid composition on SUV surface properties. Average lifetimes (A) and mole fractions (B) of C_6-NBD-PC partitioned into PC/PE/SM/CH (35/30/15/20) (circles), PC/SM/CH (65/15/20) (triangles), and PC/PE (54/46) (squares) SUVs as a function of lipid/probe molar ratio. The sum of the mole fractions of the two longer lifetime components is taken as the mole fraction of the probe partitioned into the membrane (X_{mem}).

X-ray Diffraction Studies of MLV To Monitor Interbilayer Distance. In 5% PEG, the lamellar repeat period of both PC/SM/CH (65/15/20 molar ratio) and PC/PE/SM/CH (35/30/15/20 molar ratio) was 62 Å. The lamellar repeat period contains the width of both the bilayer and the fluid space between adjacent bilayers. Thus, to determine the width of the fluid spaces between bilayers, it is necessary to determine the bilayer thickness for each system. However, since only 2 orders of lamellar diffraction were recorded, it was not possible to calculate electron density profiles to determine the relative widths of the bilayers. Therefore, to obtain higher resolution patterns, X-ray experiments were performed on oriented multilayers at high (98%) relative humidity atmospheres. At 98% relative humidity, the lamellar repeat periods were 55.1 and 54.6 Å for PC/SM/CH and PC/PE/SM/CH, respectively, and 4 orders of diffraction were recorded for each specimen. Electron density profiles from these samples are shown in Figure 9. For each profile the bilayer is centered at the origin. The high electron density peaks (centered at ±20 Å for each profile) correspond to the lipid headgroups, the low electron density region in the center of the bilayer corresponds to the lipid hydrocarbon chains, and the medium-density regions at the edges of the profiles correspond to

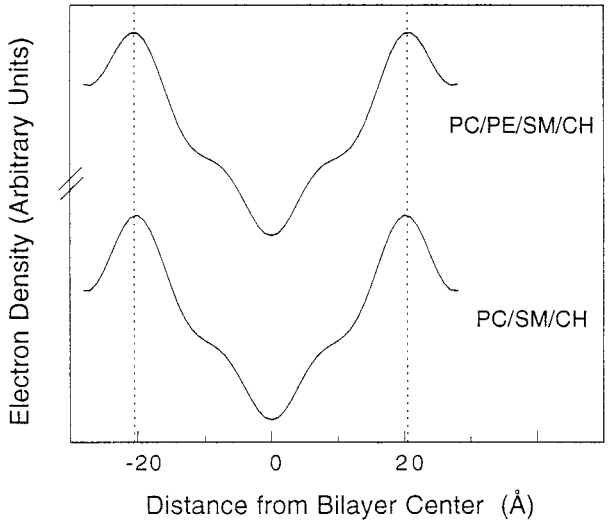

FIGURE 9: Influence of PE on interbilayer approach. Electron density profiles for lipid multilayers having a highly fusogenic composition (PC/PE/SM/CH, 35/30/15/20) and a nonfusogenic composition (PC/SM/CH, 65/15/20) at 98% relative humidity.

the fluid spaces between adjacent bilayers. The distance between the headgroup peaks was the same (40 Å) for each profile, indicating that the bilayer thickness was the same for the two lipid systems. Therefore, since the repeat periods were the same at 5% PEG, the diffraction data indicate that the interbilayer fluid spaces were approximately the same for PC/SM/CH bilayers with and without PE. We found that vesicles composed of PC/PE/SM/CH fused very well even at low PEG concentrations (3% PEG) whereas vesicles composed of PC/SM/CH did not fuse, even at 12% PEG (Figure 3). This demonstrates that inclusion of PE into PC/SM/CH bilayers helps to induce fusion by some mechanism other than by allowing closer approach of membranes.

DISCUSSION

Synthetic small, unilamellar phospholipid vesicles composed of PC/PE/SM/CH (35/30/15/20) showed an optimal ability to fuse in the presence of PEG. Except for the absence of acidic lipids such as PS and some ether-linked rather than ester-linked lipids, this composition mimics closely that of the synaptic vesicle membrane. The fact that phosphatidylserine inhibited PEG-mediated fusion in our system even in the presence of Ca^{2+} is curious, since viral fusion is regulated by negatively charged lipids (*19, 47*) and negatively charged lipids are significant components of synaptic vesicles (*48*). The role of PS in biomembrane fusion may be in binding or activating some of the several proteins that facilitate assembly of fusion complexes or that catalyze the fusion process. In addition, even low concentrations of Ca^{2+}

cause PS−Ca^{2+}−PS complex formation between bilayers brought into close opposition by other forces (*42*). Thus, PS may, through Ca^{2+}-mediated complexes, facilitate the lipid rearrangements required during the fusion process. The possible role of PS−protein interactions cannot be addressed in studies of PEG-mediated vesicle fusion, so we limited our attention to neutral lipid membranes.

Each lipid seems to have a specific role in membrane fusion. Phosphatidylethanolamine has been noted to favor Ca^{2+}-induced fusion of PC/PS LUVs (*49*) and PEG-mediated fusion of both LUVs and SUVs (*50*). PE, because of its limited headgroup hydration (*51*), may favor interbilayer close approach. However, our X-ray results show that the repeat period and fluid space between bilayers are the same for both highly fusogenic PC/PE/SM/CH and nonfusing PC/SM/CH membranes. Moreover, pure DPPC (*52*), DOPC (*53*), and mixed DOPC/SM/CH and DOPC/PE/SM (Figures 1 and 3) vesicles did not fuse at high PEG concentrations, where the fluid spacings should be quite small. Thus, we must conclude that, while close approach between monolayers clearly favors fusion (*41*), interbilayer contact seems not to be an absolute requirement for fusion.

A popular view is that membrane fusion proceeds via the formation of stalk intermediates (*54*−*57*). The energy of the stalk intermediate is highly dependent on the lipid composition of the opposed membranes. This is because different lipids tend to bend lipid monolayers in different directions, reflecting the different dynamic molecular shape of the individual lipid species, referred to as "intrinsic curvature" (*58*). It is well documented that PE has a cone-like molecular shape (small head cross section and large chain cross section) and that it promotes negative spontaneous curvature (*2*, *58*). It might be expected, therefore, that the presence of PE in the contacting monolayers of fusing membranes would reduce lipid packing and promote stalk formation and membrane merger. Our results clearly confirm this expectation. However, too high a PE content leads to a very unstable bilayer that ruptures rather than fuses (Figure 4). PE also increased water penetration and decreased lipid packing in vesicle outer leaflets (Table 2 and Figure 8). Apparently, PE promotes fusion by destabilizing the bilayer state. This effect is expected to be most pronounced in SUVs. Reduction of outer leaflet packing has been shown to favor fusion (*11*, *12*). Too much bilayer destabilization, however, promotes rupture and thus interferes with fusion. In addition, the fact that PC/PE/SM/CH and PC/SM/CH SUVs had similar outer leaflet properties (Table 2 and Figure 8) but vastly different fusogenicity (Figure 3) means that outer leaflet packing is only one feature of bilayer structure important to fusion.

Addition of cholesterol had a dramatic influence on our model membrane vesicles. Vesicles composed of PC/PE/CH were even more unstable than PC/PE vesicles and underwent mainly rupture instead of fusion (Figures 1 and 2). Vesicles composed of PC/PE/CH (43/37/20) were difficult to prepare, since they, unlike other compositions examined, aggregated and fused spontaneously (vesicle diameter changed from 38 to 54 nm over 4 h). Consistent with this, cholesterol is found to destabilize PE and PC/PE bilayers (*44*, *59*, *60*) and to induce the formation of H_{II} in preference to the lamellar phase (*61*). CH also induces negative curvature in DOPC and DOPE monolayers (*61*). Consistent with all these reports, addition of CH to PC/PE/SM SUVs made these fairly fusion-resistant membranes highly fusogenic (open squares, Figure 1). However, the role of CH must go beyond its negative intrinsic curvature, as PE also has this property and does not influence fusion as dramatically as does CH. By contrast, cholesterol had only a small effect on divalent cation-induced fusion of PS or PS/PE LUVs (*62*). This highlights the difference between PEG-mediated and cation-induced fusion of PS-rich vesicles. It is established that PEG-mediated fusion mimics the sequence of events seen in biomembrane fusion (*37*, *63*) while cation-mediated fusion does not (*64*).

Adding sphingomyelin to PC/PE vesicles dramatically reduced both fusion and rupture (open triangles and filled squares in Figure 1). In addition, vesicles composed of PC/SM/CH were nonfusogenic even at high PEG concentrations (open squares in Figure 3). Consistent with this, addition of SM to PC/PE vesicles also enhanced outer leaflet packing dramatically (Table 2 and Figure 8). It seems that the role of SM is to stabilize the lamellar state of PC/PE vesicles, thereby limiting rupture, and thus favoring nonleaky fusion. However, SM also limited fusion, so that an optimal ratio with CH (15/20) was needed to stabilize membranes against rupture without significantly limiting fusion. How might SM and CH, in an appropriate molar ratio, reduce rupture without significantly reducing contents mixing? It is well-known that SM and CH form complexes in bilayers (*7*, *8*) and that these complexes likely exist in the fluid state (*65*). Detergent-resistant domains isolated from natural (*66*) or model membranes (*6*, *65*) also contain SM and CH in a nearly 1/1 molar ratio (*7*, *8*), suggesting that SM/CH complexes form stable, well-packed lamellar structures. The dramatic effect of SM/CH ratio on efficiency of fusion (Figure 6, inset) suggests that SM/CH complexes may also be important in minimizing rupture while maximizing fusion. The dramatic drop in fusion while maintaining constant resistance to rupture at SM/CH > 3/4 (see Figure 6) suggests that some free cholesterol should exist for efficient fusion.

Since fusion involves multiple lipid rearrangements and at least two intermediates (*67*), there are a variety of ways that different lipids can contribute to fusion. Much of our discussion to this point has focused on how different lipid classes or complexes between lipids from different classes might alter bilayer packing, which probably influences mainly the first step of the process and thus shifts the balance between fusion and rupture. However, our characterization of bilayer packing and water penetration in different lipid mixtures makes it clear that factors other than outer leaflet packing and water penetration contribute significantly to fusion. Thus, the dramatic effect that addition of CH had on fusogenicity of PC/PE/SM SUVs (Figure 5) was not likely due to the effect of CH on outer leaflet stress. Indeed, PC/PE/SM/CH membranes had somewhat better packed outer leaflets than PC/PE/SM SUVs (Table 2 and Figure 8). These results clearly indicate that PC/PE/SM/CH membrane bilayers are very tight but still are optimally fusogenic. Thus, while our results make clear the importance of CH in determining the balance between rupture and fusion, the mechanistic role played by CH in fusion is still not clear. It may be that CH's low polarity allows it to redistribute across a bilayer more easily than the more polar phospholipids, thus facilitating interconversion of the first and second fusion intermediates (*37*). Alternatively, the ability of CH to form complexes with PC and SM (*3*, *68*) might destabilize

membranes rich in PE. Given the importance of CH in several viral fusion systems (*69*, *70*), it is important that its role be further investigated.

ACKNOWLEDGMENT

We thank Dr. Vladimir Malinin for many useful discussions and for much useful advice during the course of this investigation.

REFERENCES

1. White, J. M. (1992) *Science 258*, 917−924.
2. Chernomordik, L. (1996) *Chem. Phys. Lipids 81*, 203−213.
3. Lentz, B. R., Hoechli, M., and Barenholz, Y. (1981) *Biochemistry 20*, 6803−6809.
4. Xu, X., and London, E. (2000) *Biochemistry 39*, 843−849.
5. Simons, K., and Ikonen, E. (1997) *Nature 387*, 569−572.
6. Schroeder, R., London, E., and Brown, D. (1994) *Proc. Natl. Acad. Sci. U.S.A. 91*, 12130−12134.
7. Needham, D., and Nunn, R. S. (1990) *Biophys. J. 58*, 997−1009.
8. McIntosh, T. J., Simon, S. A., Needham, D., and Huang, C. H. (1992) *Biochemistry 31*, 2012−2020.
9. Raffy, S., and Teissie, J. (1999) *Biophys. J. 76*, 2072−2080.
10. Wilschut, J., Duzgunes, N., Hoekstra, D., and Papahadjopoulos, D. (1985) *Biochemistry 24*, 8−14.
11. Wu, H., Zheng, L., and Lentz, B. R. (1996) *Biochemistry 35*, 12602−12611.
12. Lee, J., and Lentz, B. R. (1997) *Biochemistry 36*, 421−431.
13. Nir, S., Wilschut, J., and Bentz, J. (1982) *Biochim. Biophys. Acta 688*, 275−278.
14. Lentz, B. R., Carpenter, T. J., and Alford, D. R. (1987) *Biochemistry 26*, 5389−5397.
15. Leikin, S., Kozlov, M. M., Fuller, N. L., and Rand, R. P. (1996) *Biophys. J. 71*, 2623−2632.
16. Duzgunes, N., Allen, T. M., Fedor, J., and Papahadjopoulos, D. (1987) *Biochemistry 26*, 8435−8442.
17. Ellens, H., Siegel, D. P., Alford, D., Yeagle, P. L., Boni, L., Lis, L. J., Quinn, P. J., and Bentz, J. (1989) *Biochemistry 28*, 3692−3703.
18. Stegmann, T., Bartoldus, I., and Zumbrunn, J. (1995) *Biochemistry 34*, 1825−1832.
19. Rafalski, M., Lear, J. D., and DeGrado, W. F. (1990) *Biochemistry 29*, 7917−7922.
20. Phalen, T., and Kielian, M. (1991) *J. Cell Biol. 112*, 615−623.
21. Wilschut, J., Corver, J., Nieva, J. L., Bron, R., Moesby, L., Reddy, K. C., and Bittman, R. (1995) *Mol. Membr. Biol. 12*, 143−149.
22. Asano, K., and Asano, A. (1988) *Biochemistry 27*, 1321−1329.
23. Yamada, S., and Ohnishi, S. (1986) *Biochemistry 25*, 3703−3708.
24. Smit, J. M., Bittman, R., and Wilschut, J. (1999) *J. Virol. 73*, 8476−8484.
25. Brock, T. G., Nagaprakash, K., Margolis, D. I., and Smolen, J. E. (1994) *J. Membr. Biol. 141*, 139−148.
26. Martin, I., Defrise-Quertain, F., Mandieau, V., Nielsen, N. M., Saermark, T., Burny, A., Brasseur, R., Ruysschaert, J. M., and Vandenbranden, M. (1991) *Biochem. Biophys. Res. Commun. 175*, 872−879.
27. Martin, I., and Ruysschaert, J. M. (1997) *FEBS Lett. 405*, 351−355.
28. Chen, P. S., Jr., Toribara, T. Y., and Warner, H. (1956) *Anal. Chem. 28*, 1756−1758.
29. Schwenk, E., and Werthessen, N. T. (1952) *Arch. Biochem. Biophys. 40*, 334−341.
30. Lentz, B. R., McIntyre, G. F., Parks, D. J., Yates, J. C., and Massenburg, D. (1992) *Biochemistry 31*, 2643−2653.
31. Lentz, B. R., Barenholz, Y., and Thompson, T. E. (1976) *Biochemistry 15*, 4529−4537.
32. Hope, M. J., Bally, M. B., Webb, G., and Cullis, P. R. (1985) *Biochim. Biophys. Acta 812*, 55−65.
33. Mayer, L. D., Hope, M. J., and Cullis, P. R. (1986) *Biochim. Biophys. Acta 858*, 161−168.
34. Wilschut, J., Duzgunes, N., Fraley, R., and Papahadjopoulos, D. (1980) *Biochemistry 19*, 6011−6021.
35. Talbot, W. A., Zheng, L. X., and Lentz, B. R. (1997) *Biochemistry 36*, 5827−5836.
36. Horrocks, W. D., Jr., and Sudnick, D. R. (1979) *J. Am. Chem. Soc. 101*, 334−340.
37. Lee, J., and Lentz, B. R. (1997) *Biochemistry 36*, 6251−6259.
38. Stryer, L. (1966) *J. Am. Chem. Soc. 88*, 5708−5712.
39. Blaurock, A. E., and Worthington, C. R. (1966) *Biophys. J. 6*, 305−312.
40. Herbette, L., Marquardt, J., Scarpa, A., and Blasie, J. K. (1977) *Biophys. J. 20*, 245−272.
41. Burgess, S. W., McIntosh, T. J., and Lentz, B. R. (1992) *Biochemistry 31*, 2653−2661.
42. Feigenson, G. W. (1989) *Biochemistry 28*, 1270−1278.
43. Stubbs, C. D., Ho, C., and Slater, S. J. (1995) *J. Fluoresc. 5*.
44. Simon, S. A., McIntosh, T. J., and LaTorre, R. (1982) *Science 216*, 65−67.
45. Chattopadhyay, A., and London, E. (1987) *Biochemistry 26*, 39−45.
46. Slater, S. J., Kelly, M. B., Taddeo, F. J., Ho, C., Rubin, E., and Stubbs, C. D. (1994) *J. Biol. Chem. 269*, 4866−4871.
47. Nieva, J. L., Nir, S., Muga, A., Goni, F. M., and Wilschut, J. (1994) *Biochemistry 33*, 3201−3209.
48. Deutsch, J. W., and Kelly, R. B. (1981) *Biochemistry 20*, 378−385.
49. Duzgunes, N., Wilschut, J., Fraley, R., and Papahadjopoulos, D. (1981) *Biochim. Biophys. Acta 642*, 182−195.
50. Yang, Q., Guo, Y., Li, L., and Hui, S. W. (1997) *Biophys. J. 73*, 277−282.
51. Marra, J., and Israelachvili, J. (1985) *Biochemistry 24*, 4608−4618.
52. Lentz, B. R., Wu, J. R., Sorrentino, A. M., and Carleton, J. N. (1991) *Biophys. J. 60*, 942−951.
53. Burgess, S. W., Massenburg, D., Yates, J., and Lentz, B. R. (1991) *Biochemistry 30*, 4193−4200.
54. Kozlov, M. M., Leikin, S. L., Chernomordik, L. V., Markin, V. S., and Chizmadzhev, Y. A. (1989) *Eur. Biophys. J. 17*, 121−129.
55. Chernomordik, L. V., Melikyan, G. B., and Chizmadzhev, Y. A. (1987) *Biochim. Biophys. Acta 906*, 309−352.
56. Chernomordik, L., Kozlov, M. M., and Zimmerberg, J. (1995) *J. Membr. Biol. 146*, 1−14.
57. Siegel, D. P. (1993) in *Viral Fusion Mechanisms* (Bentz, J., Ed.) pp 475−512, CRC Press, Inc., Boca Raton, FL.
58. Gruner, S. M. (1985) *Proc. Natl. Acad. Sci. U.S.A. 82*, 3665−3669.
59. Tilcock, C. P. S., Hope, M. J., and Cullis, P. R. (1984) *Chem. Phys. Lipids 35*, 363−370.
60. Cullis, P. R., and De Kruijff, B. (1978) *Biochim. Biophys. Acta 507*, 207−218.
61. Chen, Z., and Rand, R. P. (1997) *Biophys. J. 73*, 267−276.
62. Shavnin, S. A., Pedroso de Lima, M. C., Fedor, J., Wood, P., Bentz, J., and Duzgunes, N. (1988) *Biochim. Biophys. Acta 946*, 405−416.
63. Lee, J., and Lentz, B. R. (1998) *Proc. Natl. Acad. Sci. U.S.A. 95*, 9274−9279.
64. Rosenberg, J., Duzgunes, N., and Kayalar, C. (1983) *Biochim. Biophys. Acta 735*, 173−180.
65. Ahmed, S. N., Brown, D. A., and London, E. (1997) *Biochemistry 36*, 10944−10953.
66. Brown, D. A., and Rose, J. K. (1992) *Cell 68*, 533−544.
67. Lentz, B. R., and Lee, J. K. (2000) *Mol. Membr. Biol. 16*, 279−296.
68. Straume, M., and Litman, B. J. (1987) *Biochemistry 26*, 5121−5126.
69. Konopka, K., Davis, B. R., Larsen, C. E., Alford, D. R., Debs, R. J., and Duzgunes, N. (1990) *J. Gen. Virol. 71*, 2899−2907.
70. Larsen, C. E., Nir, S., Alford, D. R., Jennings, M., Lee, K. D., and Duzgunes, N. (1993) *Biochim. Biophys. Acta 1147*, 223−236.

BI002030K